Bicollimated Near-Field Gregorian Reflector Antenna

J. B. L. RAO

Electromagnetics Branch
Radar Division

February 9, 1983

NAVAL RESEARCH LABORATORY
Washington, D.C.

REPORT DOCUMENTATION PAGE		READ INSTRUCTIONS BEFORE COMPLETING FORM
1. REPORT NUMBER NRL Report 8658	2. GOVT ACCESSION NO. AD-A125 197	3. RECIPIENT'S CATALOG NUMBER
4. TITLE (and Subtitle) BICOLLIMATED NEAR-FIELD GREGORIAN REFLECTOR ANTENNA		5. TYPE OF REPORT & PERIOD COVERED Interim report on a continuing NRL problem.
		6. PERFORMING ORG. REPORT NUMBER
7. AUTHOR(s) J.B.L. Rao		8. CONTRACT OR GRANT NUMBER(s)
9. PERFORMING ORGANIZATION NAME AND ADDRESS Naval Research Laboratory Washington, DC 20375		10. PROGRAM ELEMENT, PROJECT, TASK AREA & WORK UNIT NUMBERS NRL Problem 53-0624 61153N; RR0210543
11. CONTROLLING OFFICE NAME AND ADDRESS Naval Electronics Systems Command Washington, DC 20350		12. REPORT DATE February 9, 1983
		13. NUMBER OF PAGES 15
14. MONITORING AGENCY NAME & ADDRESS(if different from Controlling Office)		15. SECURITY CLASS. (of this report) UNCLASSIFIED
		15a. DECLASSIFICATION/DOWNGRADING SCHEDULE

16. DISTRIBUTION STATEMENT (of this Report)

Approved for public release; distribution unlimited.

17. DISTRIBUTION STATEMENT (of the abstract entered in Block 20, if different from Report)

18. SUPPLEMENTARY NOTES

19. KEY WORDS (Continue on reverse side if necessary and identify by block number)

Reflector antenna   Ray tracing
Bicollimated reflector antenna
Limited scan antenna
Shaped dual reflector antenna

20. ABSTRACT (Continue on reverse side if necessary and identify by block number)

A bicollimated near-field Gregorian reflector is structurally similar to a classical confocal parabolic reflector, but its surfaces are shaped to have better scan capability. A geometrical optics procedure is used in designing the reflector surfaces. A three-dimensional ray tracing procedure is used in analyzing the aperture phase errors as the beam is scanned to different angles. The results show that the bicollimated configuration has about 45% greater angular scanning range than the corresponding confocal parabolic dual-reflector system.

DD $_{1\ JAN\ 73}^{FORM}$ 1473   EDITION OF 1 NOV 65 IS OBSOLETE
S/N 0102-014-6601

CONTENTS

BICOLLIMATED NEAR-FIELD GREGORIAN
REFLECTOR ANTENNA

INTRODUCTION

It is known that the bifocal dual reflector antenna [1] and bifocal dielectric lens antennas [2,3] have wider angle scan capability than their single focus counterparts. We propose a bicollimated near-field Gregorian reflector antenna which has a better scan capability compared to a classical near-field Gregorian reflector antenna [4]. The design presented applies to both symmetric or offset [5] configurations. However, only the offset configuration, which eliminates feed blockage, will be used.

The bicollimated reflector is obtained by first designing a bicollimated cylindrical reflector system using geometrical optics techniques and then revolving the cross section curves to form a surface of revolution. Selected parts of these surfaces will form an offset reflector configuration. Figure 1 shows the cross section of an offset configuration of a bicollimated near-field Gregorian reflector antenna. The cross sections of the main and subreflector are designed so that when the feed array is scanned to an angle β, the main beam is pointed to an angle $-\alpha$ relative to the reflector axis. These rays are shown, in Fig. 1, by solid lines. Similarly, when the feed array is scanned to an angle $-\beta$, the main beam is required to be pointed to an angle α, as shown by the dotted lines in Fig. 1. It is shown later in this report that only a series of points and slopes (or tangents) at those points on the cross sections of the reflector can be obtained. Using these data, the reflector cross sections are represented completely by best fit polynomials. This polynomial representation is used in computing the aperture phase errors when the antenna beam is scanned to different angles by scanning the feed array. The results showed that the bicollimated configuration has about 45% more scanning range than the corresponding confocal parabolic configuration.
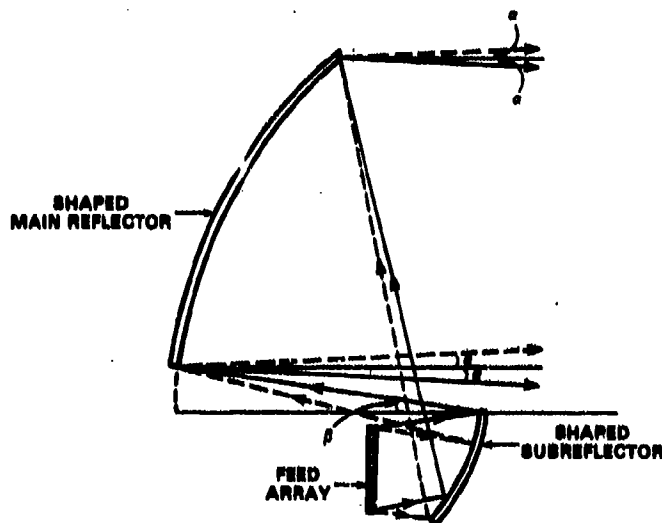

Fig. 1 — Cross section of bicollimated near-field
Gregorian reflector

1

DESIGN PROCEDURE

Figure 2 shows the cross section in the XZ-plane of an offset, bicollimated, nearfield Gregorian reflector antenna. The Z-axis is the antenna axis of rotational symmetry. The feed array is assumed to be located in the XY-plane. It is also assumed that the subreflector intersects the Z-axis at $Z = P$. From symmetry, it is evident that the subreflector is perpendicular to the Z-axis at $Z = P$. The reflected phase front B corresponds to the incident phase front A. For perfect collimation, the path length between these two phase fronts should be constant and is assumed to be L. Similarly, the path length between the phase fronts C and D is also equal to L.
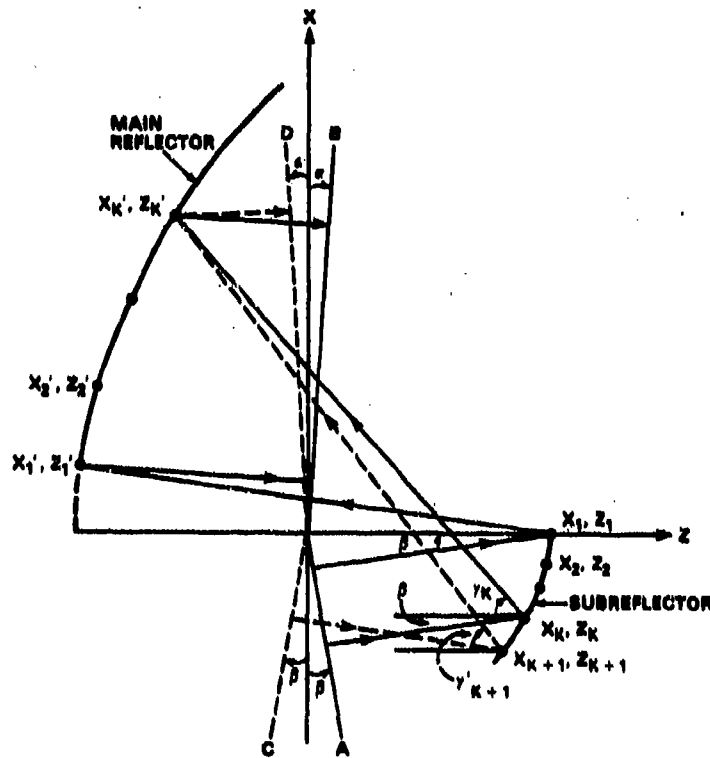

Fig. 2 — Geometry of an offset bicollimated
Gregorian reflector

Knowing the initial point (X_1, Z_1) and the slope at that point on the subreflector, one can determine the main reflector point (X_1', Z_1') and the slope at that point by applying geometrical optics principles. Next, from this known point (X_1', Z_1') and the slope on the main reflector, one can determine a point (X_2, Z_2) and the corresponding slope on the subreflector. By continuing this process a series of points and slopes on the reflector surfaces are found in succession. The pertinent results are given by two sets of formulas. The first gives a point (X_k', Z_k') and the slope at that point on the main reflector when a point (X_k, Z_k) and the corresponding slope on the subreflector are known. The relations (obtained by tracing the rays emanating from phase front A) are:

$$Z_k' = \frac{R_k - L + Z_k W - X_k \sin \alpha}{W + \cos \alpha}, \tag{1}$$

$$X_k' = X_k + (Z_k - Z_k') \tan \gamma_k, \tag{2}$$

$$(dz'/dx')_{Z_k', X_k'} = \tan \left(\frac{\gamma_k + \alpha}{2} \right), \tag{3}$$

2

where

$$R_k = Z_k \cos \beta + X_k \sin \beta, \qquad (4)$$

$$\gamma_k = \gamma_k' + 2\beta, \qquad (5)$$

and

$$W = \frac{1 + \sin \gamma_k \sin \alpha}{\cos \gamma_k}. \qquad (6)$$

In addition, Z_k, X_k, and γ_k' are given by Eqs. (7), (8), and (11) for $k \geqslant 2$. The initial values, for $k = 1$, are $Z_1 = P$ and $X_1 = 0$. From Fig. 2 it can be noted that $\gamma_1 = \beta$. Therefore, γ_1' is not needed in Eq. (5) to find γ_1.

The second set gives a point (Z_{k+1}, X_{k+1}) and the slope at that point on the subreflector when a point (X_k', Z_k') and the slope at the point on the main reflector are known. These relations (obtained by tracing the rays emanating from phase front C, Fig. 2) are:

$$Z_{k+1} = \frac{L - R_k' + Z_k' W' + X_k' \sin \beta}{W' + \cos \beta}, \qquad (7)$$

$$X_{k+1} = X_k' + (Z_k' - Z_{k+1}) \tan \gamma_{k+1}' \qquad (8)$$

$$(dz/dx)_{Z_{k+1}, X_{k+1}} = \tan \left[\frac{\gamma_{k+1}' + \beta}{2} \right], \qquad (9)$$

where

$$R_k' = -Z_k' \cos \alpha - X_k' \sin \alpha, \qquad (10)$$

$$\gamma_{k+1}' = \gamma_k + 2\alpha, \qquad (11)$$

and

$$W' = \frac{1 + \sin \gamma_{k+1}' \sin \beta}{\cos \gamma_{k+1}'}. \qquad (12)$$

Starting with the initial point (X_1, Z_1) and the angle $\gamma_1(= \beta)$, and making use of the first and then the second set of formulas and continuing the process, a series of points and slopes on each reflector surface can be found in succession.

POLYNOMIAL APPROXIMATION

The design procedure discussed in the previous section gives a finite number of points and an equal number of slopes on the reflector surfaces. In order to define the reflector surfaces completely, it is necessary to use an approximation. It is convenient to approximate the reflector cross sections by best fit polynomials. Since the reflectors are axially symmetric, only even powers are required. The reflector cross sections are represented by the polynomials

$$Z_s = B_0 + B_1 X_s^2 + B_2 X_s^4 + \ldots, \qquad (13)$$

$$Z_m = A_0 + A_1 X_m^2 + A_2 X_m^4 + \ldots, \qquad (14)$$

where X_s and Z_s are the subreflector coordinates, and X_m and Z_m are the main reflector coordinates.

If the number of data points available limits the degree of the polynomial, the known slopes on the reflector curves can be used to improve the accuracy.

EQUIVALENT NEAR-FIELD GREGORIAN REFLECTOR

To compare the performance of the bicollimated reflector antenna, it is necessary to define an equivalent confocal reflector system. The equivalence is established here by making the magnification M of the confocal reflector equal to β/α and make the path-length between the incident and the radiating wavefronts equal to L for an on-axis beam for the confocal reflector. In addition, the subreflector is assumed to be at the same distance P from the origin as in the bicollimated case. The first condition gives the following relationships:

$$F_m/F_s = M = \beta/\alpha, \tag{15}$$

where F_m and F_s are the focal lengths of the main and subreflector of an equivalent confocal reflector.

The second condition gives the following:

$$F_m + F_s = L/2. \tag{16}$$

Solving for F_m and F_s from (15) and (16), we have

$$F_s = L/2 \, (M + 1),$$

$$F_m = ML/2(M + 1).$$

Therefore, the equivalent parabolic subreflector is given by the equation

$$Z_{sp} = P - \frac{1 + M}{2L} X_{sp}^2, \tag{19}$$

and the equivalent parabolic main reflector is given by

$$Z_{mp} = (L/2) - P - \frac{1 + M}{2LM} X_{mp}^2. \tag{20}$$

There are other ways of defining an equivalent confocal reflector. However, there is no need to find precise equivalence (if there is such a thing) because small changes in the Gregorian antenna parameters do not appreciably influence its scanning performance as long as the confocal conditions is not violated. Another point which should be noted is that at the outset it may appear that an equivalent confocal reflector can be obtained simply by taking the first two terms in the polynomial representation of the bicollimated reflector. However, the main and subreflectors so obtained will not form a confocal set.

PHASE ERROR ANALYSIS

In the classical near-field Gregorian system [5], it is known that the amplitude distribution applied to the feed array is reproduced over the main aperture without alteration. For values of α which are of practical interest, the bicollimated reflector system does not deviate much from an equivalent classical near-field Gregorian system. Therefore, it is reasonable to assume that the main aperture amplitude distribution is the same as that of the feed array. However, the aperture phase errors are different in the two systems. The purpose of this section is to analyze the aperture phase errors and show the advantages of the bicollimated reflector system. Figure 3 shows the geometry used in analyzing the aperture phase errors. The aperture phase errors are found by assuming that a plane wave is incident on the main reflector at an angle θ and ϕ, which also corresponds to the mainbeam direction. Path-length errors on the aperture are determined from the path-length between the incident wavefront and the corresponding feed array wavefront, as discussed in the appendix of this report. Equation (A23) gives the path-length error on the aperture. The procedure given in the appendix applies to both bicollimated and confocal reflector antennas.
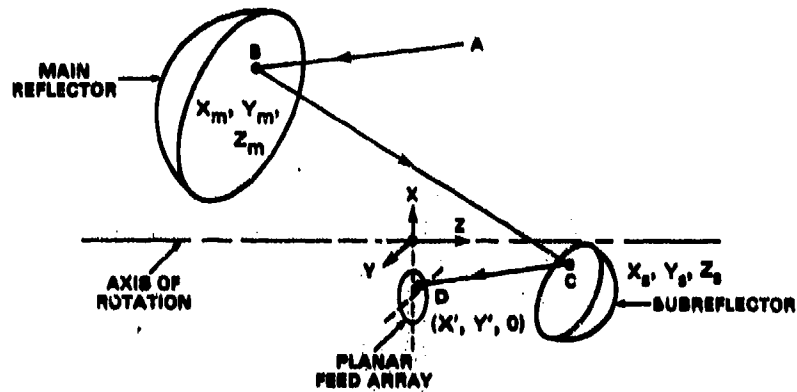
4

Fig. 3 — Path of general ray used in 3-D ray
tracing method

NUMERICAL EXAMPLE

As an example, a bicollimated reflector antenna is designed with $\alpha = 3°$, $\beta = 9°$, and $L/P = 2.5$. Table 1 gives computed data points.

Table 1 — Computed Points on the Reflector
Cross Sections

Z_s/P	X_s/P	Z_m/P	X_m/P
1.000000	0	−0.24342	0.196938
0.985926	−0.132464	−0.154958	0.608434
0.938416	−0.276962	0.057515	1.079506
0.836951	−0.450222	0.49982	1.678324

By use of the data points shown in Table 1, the reflector cross sections are approximated by the following best fit polynomial representation:

$$z_s = 0.999998 - 0.8018732 \, x_s^2 - 0.01234972 \, x_s^4, \tag{21}$$

$$z_m = 0.253768 + 0.26682 \, x_m^2 + 0.00025741 \, x_m^4, \tag{22}$$

where

$$z_s = Z_s/P, \quad x_s = X_s/P, \quad z_m = Z_m/P \text{ and } x_m = X_m/P.$$

Reflector surfaces are obtained by rotating the above cross sections about the Z-axis and choosing only selected parts. Figure 4 shows the geometry and the antenna parameters of the offset bicollimated reflector which is chosen as an example. The main reflector surface is chosen so that it is circular when projected into the XY-plane. The main aperture is assumed to be completely utilized over the scanning range of interest. The corresponding illuminated areas of the feed array and the subreflector surface may change with scan angle. For the example under consideration, the main reflector diameter $D = 1.6P$ and the main reflector is offset from the Z-axis by $0.3P$ to eliminate blockage due to the subreflector when the beam is scanned below the Z-axis.

By use of the $3D$ ray tracing method developed in the appendix, a computer program is devised to determine the aperture phase errors when the beam is scanned to different scan angles. Using that program, it is possible to obtain path-length errors over the whole aperture. However, Fig. 5 shows these errors on the aperture in one plane (XZ-plane) only as the errors are similar in other planes. The solid
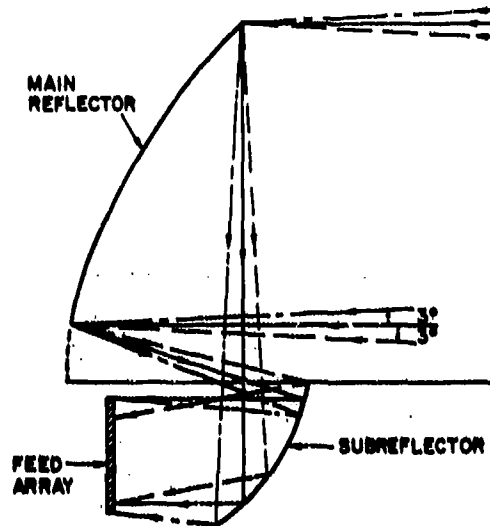
5

Fig. 4 — Cross section of the bicollimated reflector
designed with $\alpha = 3°$, $\beta = 9°$ and $L = 2.5$ P
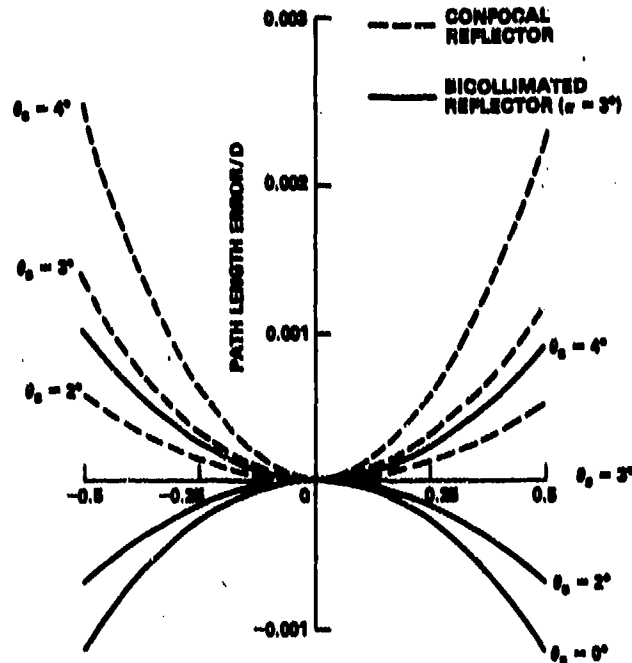

Fig. 5 — Aperture phase errors in XZ-plane

curves belong to the bicollimated reflector. As expected, the aperture errors for $\theta_s = 3°$ ($\alpha = 3°$) are zero. However, for $\theta_s = 0$ (on axis beam) the biocollimated reflector has aperture errors whose magnitude increases toward the edges of the aperture. For comparison, aperture errors are computed for an equivalent confocal reflector and are shown as dashed curves in Fig. 5. For the confocal reflector, the aperture errors are zero for $\theta_s = 0$ and increases with θ_s. The maximum errors appear towards the edges of the aperture.

For each scan angle, the maximum error on the aperture is determined by using the data shown in Fig. 5 and similar data obtained for other planes. This maximum path-length error normalized to aperture diameter is plotted in Fig. 6 as a function of the scan angle when the main beam is scanned in $\phi = 0$ plane. For the confocal reflector, the maximum path-length error increases monotonically with the scan angle whereas the path-length error for the bicollimated reflector decreases with the scan angle and becomes zero for $\theta = \alpha$ (3° in the example) and then increases monotonically with the scan angle. For a maximum normalized path-length error of 0.0011, Fig. 6 shows that the confocal reflector can be scanned up to 2.7° and the bicollimated reflector can be scanned up to 4°. Therefore, the bicollimated reflector has about 48% more scanning range in $\phi = 0$ plane than the scanning range of an equivalent confocal reflector. Figures 7 and 8 show similar results for scanning in $\phi = 90°$ and 180° planes. Figure 9 shows the complete scanning ranges, for a maximum normalized path-length error of 0.0011, for both confocal and bicollimated reflector antennas. The results show that the bicollimated reflector has about 45% more scanning range than an equivalent confocal reflector.

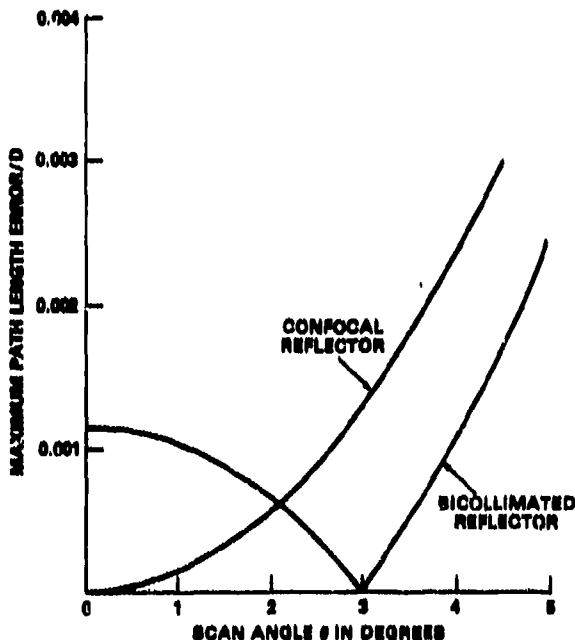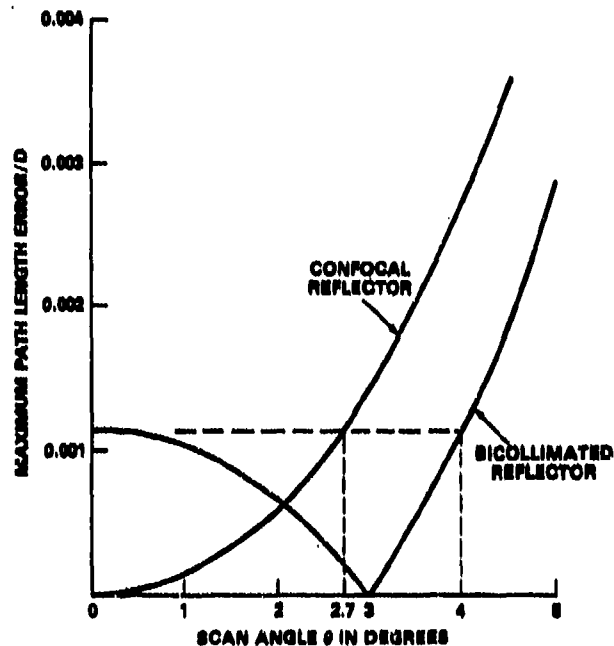Fig. 6 — Maximum error on the aperture when scanned in $\phi = 0$ plane

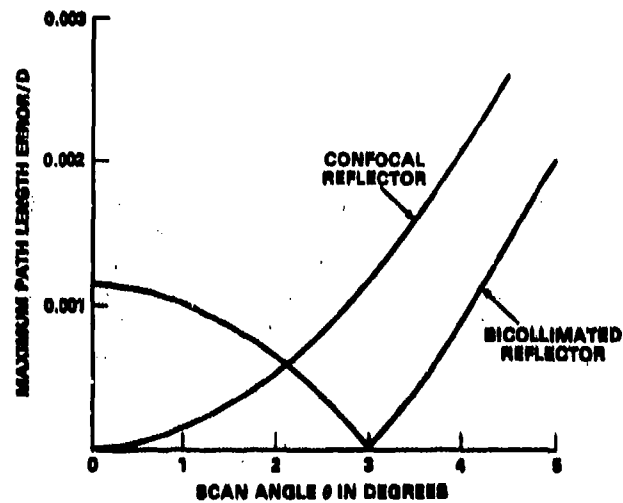Fig. 7 — Maximum error on the aperture when scanned in $\phi = 90°$ plane

7

Fig. 8 — Maximum error on the aperture when
scanned in $\phi = 180°$ plane
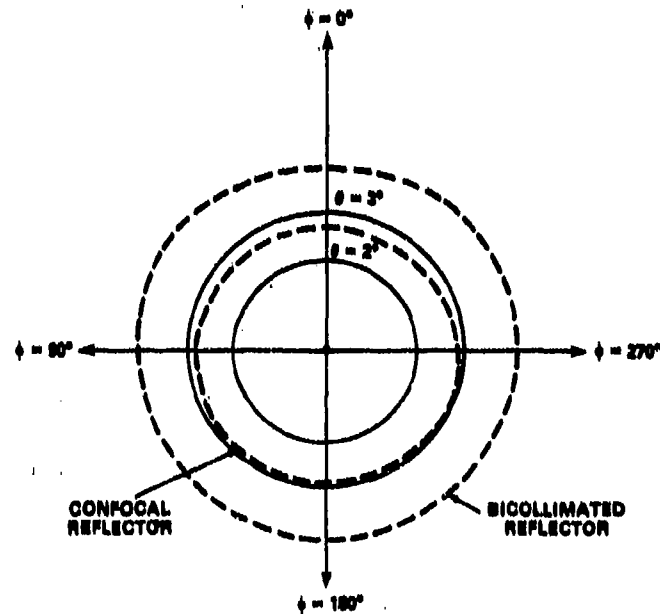
Fig. 9 — Scanning ranges for confocal and bicollimated
reflectors for maximum normalized path-length error

CONCLUSIONS

A biocollimated dual reflector antenna, which can collimate a beam in two different directions, is proposed. A design procedure is presented for determining the reflector surfaces. Aperture phase errors are analyzed for different scan angles. The results show that the bicollimated reflector has about 45% more scanning range compared to an equivalent near-field Gregorian reflector

REFERENCES

1. B.L.J. Rao, "Bifocal Dual Reflector Antennas," *IEEE Trans. on Antennas Propag.*, **AP-22**, pp. 711-714, (1974).

2. R.M. Brown, "Dielectric Bifocal Lenses," *IRE National Convention Record*, (1956), pp. 180-187.

3. F.S. Holt and A. Mayer, "A Design Procedure for Dielectric Microwave Lenses of Large Aperture Ratio and Large Scanning Angle," *IRE Trans. on Antennas and Propag.*, Jan. 1957, pp. 25-30.

4. S.P. Morgan, "Some Examples of Generalized Cassegrainian and Gregorian Antennas," *IEEE Trans. On Antennas Propag.* **AP-12**, pp. 685-691, (1964).

5. W.D. Fitzgerald, "Limited Electronic Scanning with an Offset-Feed Near-Field Gregorian System," MIT Lincoln Laboratory, Tech. Rpt. No. 486, Sept. 24, 1971.

Appendix

THREE-DIMENSIONAL RAY TRACING PROCEDURE

A ray tracing procedure is used to compute aperture phase errors for the bicollimated reflector antenna. Figure 3 of this report is used to illustrate the procedure. First we compute the path length of a general ray from a point A on the incident wave front through a point $B(X_m, Y_m, Z_m)$ on the main reflector and a point $C(X_s, Y_s, Z_s)$ on the subreflector, and finally to a corresponding point $D(X', Y')$ in the feed plane. The equation of the subreflector is assumed to be a sixth degree polynomial and is given as

$$Z_s = B_0 + B_1\rho_s^2 + B_2\rho_s^4 + B_3\rho_s^6, \tag{A1}$$

where $\rho_s = \sqrt{X_s^2 + Y_s^2}$.

Similarly, the equation of the main reflector is

$$Z_m = A_0 + A_1\rho_m^2 + A_2\rho_m^4 + A_3\rho_m^6, \tag{A2}$$

where $\rho_m = \sqrt{X_m^2 + Y_m^2}$.

The spherical coordinates θ, ϕ define the direction of the general ray incident at a known point $B(X_m, Y_m, Z_m)$ on the main reflector. This incident ray is parallel to

$$\overline{ab} = \overline{i} \sin\theta \cos\phi + \overline{j} \sin\theta \sin\phi + \overline{k} \cos\theta, \tag{A3}$$

where $\overline{i}, \overline{j}, \overline{k}$ are the unit vectors parallel to X, Y, Z coordinates and lower case letters denote unit vectors.

The length $|\overline{AB}|$, which is needed later to find the aperture phase errors, is given as

$$|\overline{AB}| = X_m \sin\theta \cos\phi + Y_m \sin\theta \sin\phi + Z_m \cos\theta. \tag{A4}$$

To find the unit vector $\overline{bc}$ of the reflected ray, Snell's law is used to relate the incident, reflected, and normal unit vectors at the point (X_m, Y_m, Z_m) on the main reflector. This is given as

$$\overline{bc} = \overline{ab} - 2\overline{n}_m(\overline{n}_m \cdot \overline{ab}), \tag{A5}$$

where $\overline{n}_m$ is the unit normal vector at the point (X_m, Y_m, Z_m) on the main reflector. By using Eq. (A2), the unit normal $\overline{n}_m$ is

$$\overline{n}_m = \frac{-\overline{i}Z_{mx} - \overline{j}Z_{my} + \overline{k}}{\sqrt{1 + Z_{mx}^2 + Z_{my}^2}}, \tag{A6}$$

where

$$Z_{mx} = \frac{\partial Z_m}{\partial X_m} = A_1(2X_m) + A_2(4X_m^3 + 4X_m Y_m^2)$$

$$+ A_3(6X_m^5 + 12X_m^3 Y_m^2 + 6X_m Y_m^4),$$

$$Z_{my} = \frac{\partial Z_m}{\partial Y_m} = A_1(2Y_m) + A_2(4Y_m^3 + 4Y_m X_m^2)$$

10

$$+ A_3(6Y_m^5 + 12Y_m^3 X_m^2 + 6Y_m X_m^4). \tag{A7}$$

The unit normal $\bar{n}_m$ can be expressed as

$$\bar{n}_m = \bar{i}\delta_x + \bar{j}\delta y + \bar{k}\delta_z, \tag{A8}$$

where

$$\delta_x = -Z_{mx}/\sqrt{1 + Z_{mx}^2 + Z_{my}^2},$$
$$\delta_y = -Z_{my}/\sqrt{1 + Z_{mx}^2 + Z_{my}^2},$$

and

$$\delta_z = 1/\sqrt{1 + Z_{mx}^2 + Z_{my}^2}.$$

Substituting for $\overline{ab}$ and $\bar{n}_m$, using Eqs. (A3) and (A8), in Eq. (A5), the unit vector $\overline{bc}$ is

$$\overline{bc} = \bar{i} R_x + \bar{j} R_y + \bar{k} R_z, \tag{A9}$$

where

$$R_x = \sin\theta \cos\phi - 2T\delta_x,$$
$$R_y = \sin\theta \sin\phi - 2T\delta_y,$$
$$R_z = \cos\theta - 2T\delta_z,$$

and $T = \bar{n}_m \cdot \overline{ab} = \delta_x \sin\theta \cos\phi + \delta_y \sin\theta \sin\phi + \delta_z \cos\theta.$

The ray $\overline{BC}$ is given by

$$\overline{BC} = \bar{i}(X_s - X_m) + \bar{j}(Y_s - Y_m) + \bar{k}(Z_s - Z_m). \tag{A10}$$

Equating the unit vectors $\overline{bc} = \overline{BC}/|\overline{BC}|$, we will have three equations defining a line in space, only two of which are independent; thus,

$$\frac{X_s - X_M}{R_x} = \frac{Y_s - Y_m}{R_y} = \frac{Z_s - Z_m}{R_z} = R, \tag{A11}$$

where $R = |\overline{BC}|$.

Equations (A11) and (A1) are solved, as outlined below, to determine the point X_s, Y_s, Z_s on the subreflector. The following can be obtained from Eq. (A11)

$$X_s = R R_x + X_m,$$
$$Y_s = R R_y + Y_m,$$
$$Z_s = R R_z + Z_m. \tag{A12}$$

Knowing R, Eq. (A12) can be used to find the point on the subreflector. First, therefore, a solution for R will be obtained by eliminating X_s, Y_s, and Z_s in Eq. (A1) by using Eq. (A12). By doing this, a sixth order equation (polynomial) in R is obtained as shown below,

$$a_6 R^6 + a_5 R^5 + a_4 R^4 + a_3 R^3 + a_2 R^2 + a_1 R + a_0 = 0, \tag{A13}$$

where

$$a_0 = A_0 + A_1 S_3 + A_2 T_5 + A_3 E_7 - Z_m,$$
$$a_1 = A_1 S_2 + A_2 T_4 + A_3 E_6 - R_z,$$
$$a_2 = A_1 S_1 + A_2 T_3 + A_3 E_5,$$

$$a_3 = A_2 T_2 + A_3 E_4,$$

$$a_4 = A_2 T_1 + A_3 E_3,$$

$$a_5 = A_3 E_2,$$

$$a_6 = A_3 E_1,$$

$$E_1 = T_1 S_1,$$

$$E_2 = T_2 S_1 + T_1 S_2,$$

$$E_3 = T_3 S_1 + T_2 S_2 + T_1 S_3,$$

$$E_4 = T_4 S_1 + T_3 S_2 + T_2 S_3,$$

$$E_5 = T_5 S_1 + T_4 S_2 + T_3 S_3,$$

$$E_6 = T_5 S_2 + T_4 S_3,$$

$$E_7 = T_5 S_3,$$

$$T_1 = S_1^2,$$

$$T_2 = 2 S_1 S_2,$$

$$T_3 = S_2^2 + 2 S_1 S_3,$$

$$T_4 = 2 S_2 S_3,$$

$$T_5 = S_3^2,$$

$$S_1 = R_x^2 + R_y^2,$$

$$S_2 = 2(R_x X_m + R_y Y_m),$$

and

$$S_3 = X_m^2 + Y_m^2.$$

Equation (A13) is used to find R by using a standard routine for solving the roots of a polynomial. In general there will be six roots for a sixth order polynomial; some are complex and some are real, with only one correct real root. A procedure is devised, using physical constraints, to select the correct root, and hence the value of R. Equation (A12) is then used to find the point (X_s, Y_s, Z_s) on the subreflector.

Next, the direction of the reflected ray $\overline{CD}$ and the length $|\overline{CD}|$ will be determined. Snell's law of reflection at the point (X_s, Y_s, Z_s) is written as

$$\overline{cd} = \overline{bc} - 2\overline{n}_s(\overline{n}_s \cdot \overline{bc}).$$ (A14)

The unit normal at the point of reflection on the subreflector is

$$\overline{n}_s = \overline{I}\alpha_x + \overline{J}\alpha_y + \overline{k}\alpha_z$$ (A15)

where

$$\alpha_x = Z_{xx}/\sqrt{1 + Z_{xx}^2 + Z_{xy}^2},$$

$$\alpha_y = Z_{xy}/\sqrt{1 + Z_{xx}^2 + Z_{xy}^2},$$

$$\alpha_z = -1/\sqrt{1 + Z_{xx}^2 + Z_{xy}^2},$$

$$Z_{xx} = \frac{\partial Z_s}{\partial X_s} = B_1(2X_s) + B_2(4X_s^3 + 4X_s Y_s^2)$$

12

$$+ B_3(6X_s^5 + 12X_s^3Y_s^2 + 6X_sY_s^4),$$

and

$$Z_{sy} = \frac{\partial Z_s}{\partial Y_s} = B_1(2Y_s) + B_2(4Y_s^3 + 4Y_sX_s^2)$$

$$+ B_3(6Y_s^5 + 12Y_s^3X_s^2 + 6Y_sX_s^4).$$

Substituting for $\overline{bc}$ and $\bar{n}_s$, using Eqs. (A9) and (A15) in Eq. (A14), the unit vector $\overline{cd}$ is

$$\overline{cd} = \overline{i}(R_x - 2Q\alpha_x) + \overline{j}(R_y - 2Q\alpha_y) + \overline{k}(R_z - 2Q\alpha_z), \tag{A16}$$

where $Q = \bar{n}_s \cdot \overline{bc} = \alpha_xR_x + \alpha_yR_y + \alpha_zR_z$. Other parameters in Eq. (A16) have been defined previously. The ray $\overline{CD}$ can also be expressed as

$$\overline{CD} = \overline{i}(X' - X_s) + \overline{j}(Y' - Y_s) + \overline{k}(-Z_s), \tag{A17}$$

where the array aperture plane is defined as the plane $Z' = 0$ and (X', Y') is the point of intersection D in the feed array plane.

The equation $\overline{cd} = \overline{CD}/|\overline{CD}|$ yields three equations; only two of them are independent, which are sufficient to determine the point of intersection (X', Y') in the aperture plane $Z' = 0$:

$$\frac{X' - X_s}{R_x - 2Q\alpha_x} = \frac{Y' - Y_s}{R_y - 2Q\alpha_y} = \frac{-Z_s}{R_z - 2Q\alpha_z},$$

from which

$$X' = X_s - \frac{(R_x - 2Q\alpha_x)Z_s}{(R_z - 2Q\alpha_z)}, \tag{A18}$$

$$Y' = Y_s - \frac{(R_y - 2Q\alpha_y)Z_s}{(R_z - 2Q\alpha_z)}, \tag{A19}$$

and

$$Z' = 0, \tag{A20}$$

the path length $|\overline{CD}|$ is

$$|\overline{CD}| = \sqrt{(X' - X_s)^2 + (Y' - Y_s)^2 + (Z' - Z_s)^2}. \tag{A21}$$

The total path length is simply the sum of the component path lengths. Hence,

$$L_0 = |\overline{AB}| + |\overline{BC}| + |\overline{CD}|. \tag{A22}$$

For an assumed direction (θ, ϕ) for the mainbeam it was noted that the direction of the rays incident on the feed array are not perfectly parallel to each other. However, an optimum phase front which minimizes aperture phase errors can be found. Let this phase front be defined by the feed steering angles θ_f and ϕ_f which are necessary to steer the mainbeam in the direction of θ and ϕ. Then, one can show that the aperture path length errors are given by

$$\Delta L = L_0 - X' \sin\theta_f \cos\phi_f - Y' \sin\theta_f \sin\phi_f - L. \tag{A23}$$